Thermal maturation and hydrocarbon migration within La Popa Basin, northeastern Mexico, with implications for other salt structures

Samuel M. Hudson and Andrew D. Hanson

ABSTRACT

Some outcrops adjacent to the 25-km (15-mi)-long salt weld in the La Popa Basin, northeastern Mexico, are visibly stained and contain enrichment of organic carbon. Their presence, which is known only along the northwestern part of the weld and along the southwestern side of the weld, provides evidence for hydrocarbon migration along the weld. This distribution is presumed to be partially controlled by the restricted distribution of the source rock that generated the hydrocarbons within the salt-withdrawal basin southwest of the weld but may have been in part controlled by a previously existing salt wall, or the weld that formed as a result of salt evacuation, acting as a barrier to lateral migration and serving as a vertical conduit for fluid flow. Upturned halokinetic strata adjacent to the weld provided a conduit for migration along bedding planes. Although no flowing seeps were seen during this study, we documented discoloration and remineralization, as well as the presence of waxy-appearing soil that smelled like crude oil at some sites near the weld. Organic geochemical analyses confirm the presence of nonbiodegraded hydrocarbons along the salt-sediment interface and within adjacent, upturned lithologies up to 5 m (16 ft) southwest of the weld. The results document for the first time the definitive presence of actively migrating hydrocarbons associated with a subaerial salt weld. An oil-source rock correlation is inferred with the upper mudstone member of the Potrerillos Formation based on biomarker data. Thermal and subsidence modeling of the basin indicate that all of the strata in the basin

Manuscript received January 26, 2007; provisional acceptance April 17, 2007; revised manuscript received April 9, 2009; final acceptance July 13, 2009.
DOI:10.1306/07130907012

AUTHORS

Samuel M. Hudson ~ *Department of Geoscience, University of Nevada Las Vegas, 4505 South Maryland Parkway, Las Vegas, Nevada 89154-4010; present address: ConocoPhillips, Houston, Texas 77079; Sam.M.Hudson@conocophillips.com*

Sam Hudson received his M.S. degree in geology from the University of Nevada, Las Vegas, and his Ph.D. in geology from the University of Utah. He is currently working in the subsurface technology group at ConocoPhillips. His research interests include facies and property modeling, basin analysis, and stratigraphy.

Andrew D. Hanson ~ *Department of Geoscience, University of Nevada Las Vegas, 4505 South Maryland Parkway, Las Vegas, Nevada 89154-4010; andrew.hanson@unlv.edu*

Andrew Hanson is an associate professor in the Geoscience Department at the University of Nevada, Las Vegas. His research interests include thermal maturation and hydrocarbon migration in basins impacted by salt tectonics, extensional basins within the Sevier hinterland, and Miocene–Pliocene extensional basins in the central Basin and Range. He earned degrees from Montana State, San Diego State, and Stanford University.

ACKNOWLEDGEMENTS

We thank the Institute of Tectonic Studies at New Mexico State University for major financial support for this project; the Stanford Molecular Organic Geochemistry Laboratory for discussions, support, and reduced costs of biomarker analyses; and Dan Jarvie and Humble Geochemical Services for reduced rates for the conventional geochemical analyses (TOC and Rock-Eval). Grants from the University of Nevada Las Vegas (awarded to Hanson) and the Geological Society of America (awarded to Hudson) provided additional funding. Tim Lawton, Kate Giles, Gary Gray, and Mark Rowan are thanked for sharing their vast knowledge of the geology of the La Popa Basin. Reviews by Barry Katz, Michael Hudec, and David Eby and discussions with Ken Peters resulted in significant improvements in the manuscript. Platte River Associates provided BMod 1-D (ver. 5.20) to the UNLV Geoscience Department at an academic rate. The AAPG Editor thanks the following reviewers for their work on this article: David E. Eby, Michael R. Hudec, and Barry Katz.

are mature enough to have generated hydrocarbons. The lower part of the stratigraphic section entered the gas generation window, and much of the Cretaceous section and all of the Tertiary entered the oil window prior to uplift of the basin. Significant unroofing (as much as 7 km [4.3 mi] of sediment may have been removed) occurred sometime after the Eocene, as suggested by previous studies.

INTRODUCTION

The La Popa Basin, northeastern Mexico (Figure 1), contains one of the rare subaerial exposures of diapiric salt in the western hemisphere. Salt of the Jurassic Minas Viejas Formation is currently exposed in three major structures in the basin: within two diapirs, each 4–6 km (2.4–3.7 mi) in diameter, and along sections of the approximately 25-km (15-mi)-long La Popa salt weld as shown in Figure 2 (Giles and Lawton, 1999). The La Popa Basin initiated as an isolated rift basin in the Jurassic and continued to be a depocenter until at least the Eocene, with uplift and erosion occurring after the Eocene (Gray et al., 2001; Lawton et al., 2001). As a result, the basin contains sediments ranging in age from Late Jurassic to Eocene, as shown in Figure 3 (Lawton et al., 2001). Current boundaries of the basin are topographic and are defined by several anticlinal ranges (Giles and Lawton, 1999). The basin is located in the foreland of the Sierra Madre orogen (Lawton et al., 2001) (Figure 1).

The weld in the La Popa Basin is a secondary, subvertical salt weld, which is the remnant of an evacuated salt wall (Giles and Lawton, 1999) (Figure 2). Evacuation of salt along the weld occurred as the supply of diapiric salt slowed because of evacuation at depth, which resulted in primary basement welds forming between the basin strata and the underlying basement (Giles and Lawton, 1999). The strike of the weld is west-northwest–east-southeast along its western section and northwest–southeast along its eastern section, connected by a large convex-to-the-southwest bend near the middle of its length (Giles and Lawton, 1999) (Figure 2). Up to 5 km (3.1 mi) of stratigraphic offset between juxtaposed lithologies on either side of the weld are observed (Figure 2), with the southern side of the weld being down dropped (Giles and Lawton, 1999). This offset is thought to be the result of a normal fault in the basement that also has a down-dropped southern hanging wall and places lithologies ranging in age from Late Cretaceous to middle Eocene in contact across the weld (Giles and Lawton, 1999). Although the La Popa weld is referred to as a salt weld, note that some areas along the weld contain abundant diapiric gypsum. In fact, the northwest end of the weld is a diapir (Figure 2) and salt pinches out gradually to the southeast.

One of the major issues regarding hydrocarbon interaction with salt welds is whether salt welds act as conduits or barriers (or both) to fluid migration. Within the Gulf of Mexico, previous work has led to differing opinions. McBride et al. (1998) in a study of the offshore Gulf of Mexico shelf near Louisiana stated that salt welds do not impede the vertical rise of hydrocarbons. Several other workers have claimed that salt welds “commonly separate distinct structural domains” in the Gulf of Mexico and affect hydrocarbon migration patterns (Pritchett and House, 1998, p. 1954). Welds have also been implicated in forming major components of hydrocarbon traps through juxtaposition of different strata on either side of the weld (Snyder and Nugent, 1996). Rowan (2004) pointed out that, in some cases, hydrocarbons clearly migrate through welds, whereas in other cases, welds may serve as seals.

One of the goals of this study was to determine if migrated hydrocarbons occur along the weld in the La Popa Basin. Away from the weld, samples of Jurassic–Eocene strata were gathered in an attempt to identify effective source rock(s) within the basin (Peters and Cassa, 1994), so that, in the event that migrated hydrocarbons were found along the weld, an oil-source rock correlation could be attempted. A further goal of this study was to document the thermal and subsidence history of the basin. Identification of a source rock(s), linked with subsidence and the thermal history of the basin, would allow a better understanding of (1) the timing of hydrocarbon generation, (2) the amount of salt present along the weld during hydrocarbon migration (salt weld versus salt wall), and (3) possibly the migration

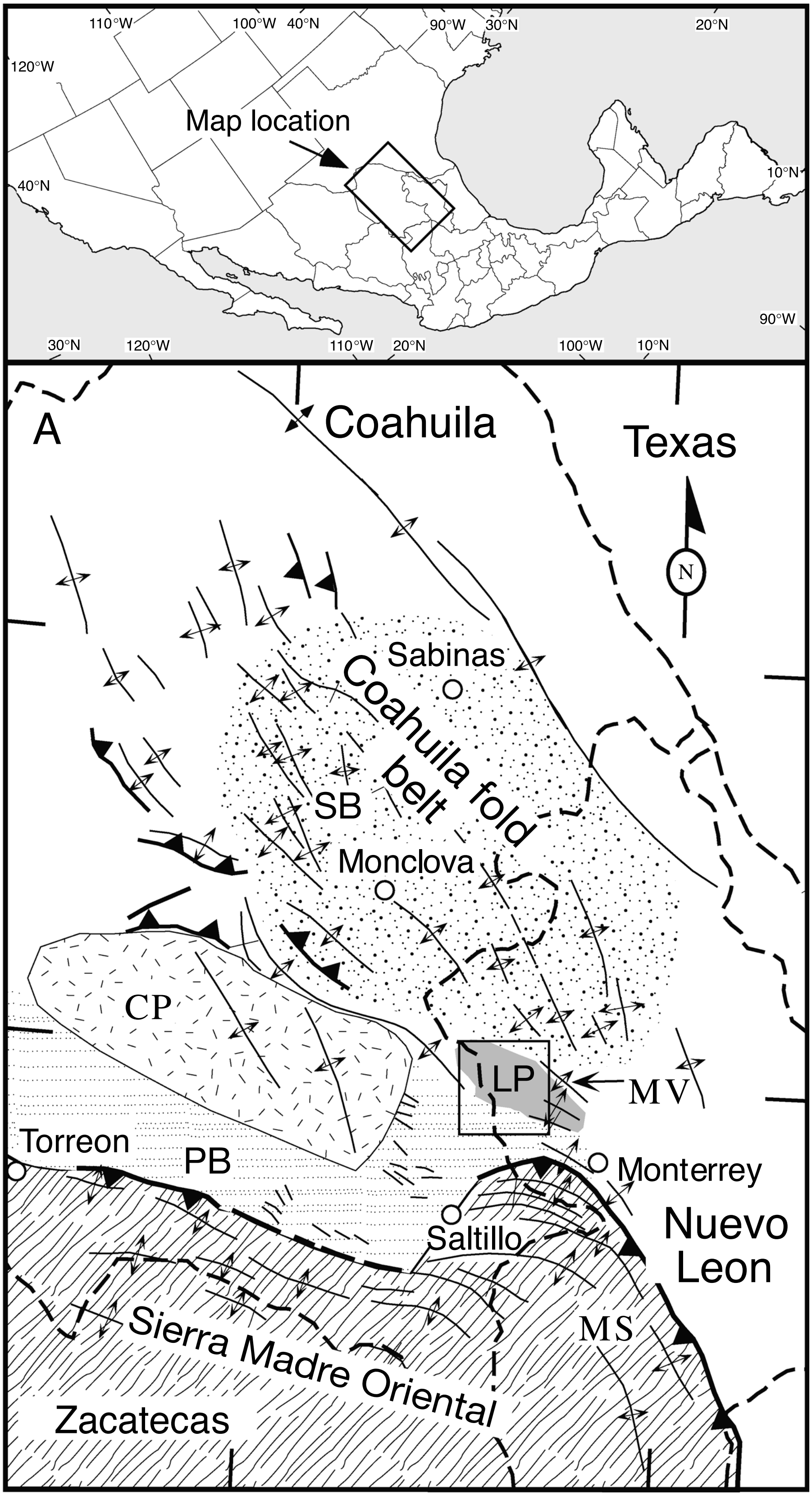

Figure 1. Location map showing the setting of the La Popa Basin (the lower map area is indicated on the upper map). LP = La Popa Basin; CP = Coahuila platform; PB = Parras Basin; MV = Minas Viejas anticline; MS = Monterrey salient; SB = Salinas Basin (modified from Lawton et al., 2001). The box on the lower map indicates Figure 2.

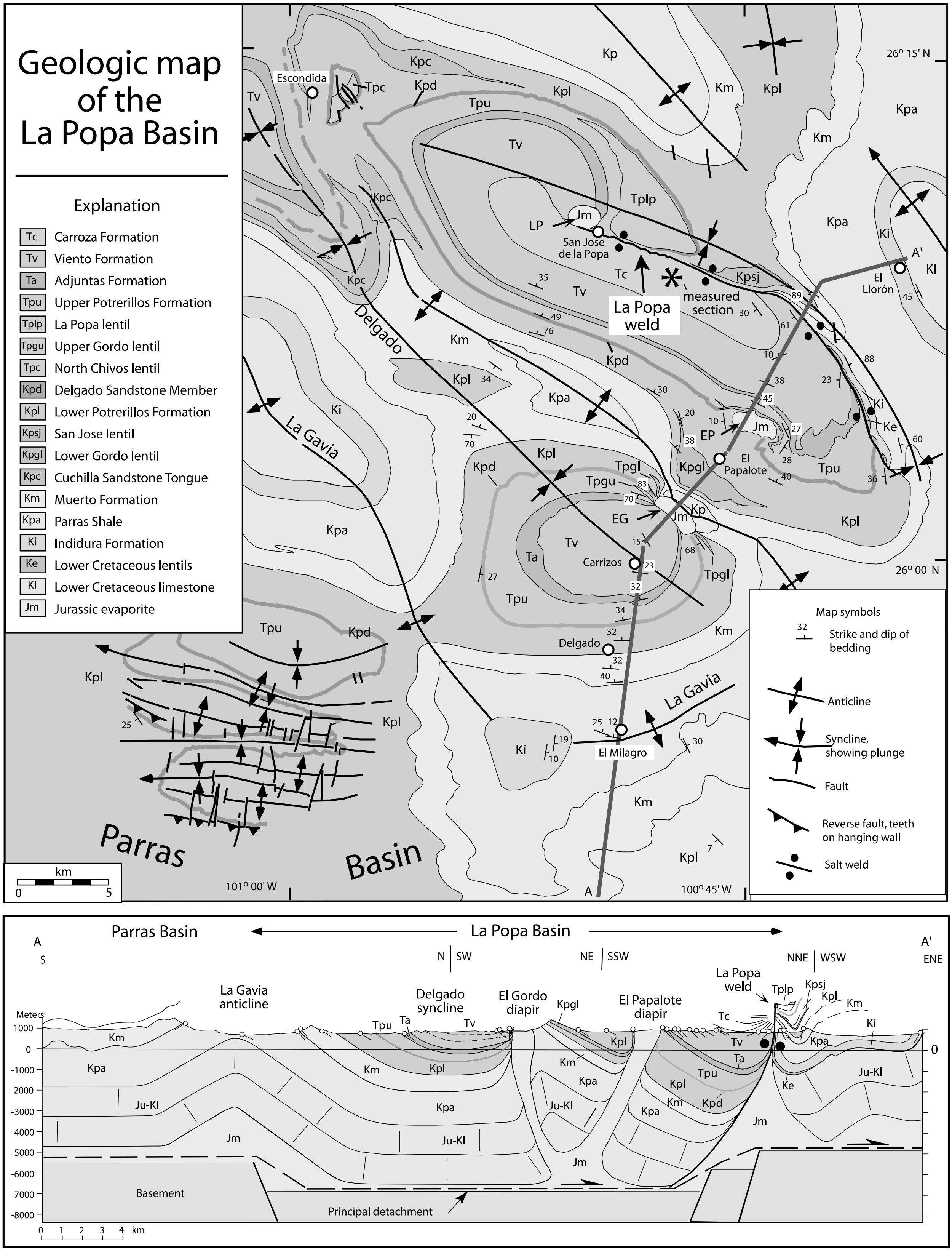

Figure 2. Geologic map and cross section of the La Popa Basin: the dashed box in the upper right indicates the area shown in Figure 4. The cross section line is labeled A-A'. The figure is modified from a section drawn by Hector Milan, University of Zaragoza, Spain (modified from Giles and Lawton, 2002). BC = Boca la Carroza; EG = El Gordo diapir; EP = El Papalote diapir; LP = La Popa diapir; Ju-Kl = Upper Jurassic-Lower Cretaceous.

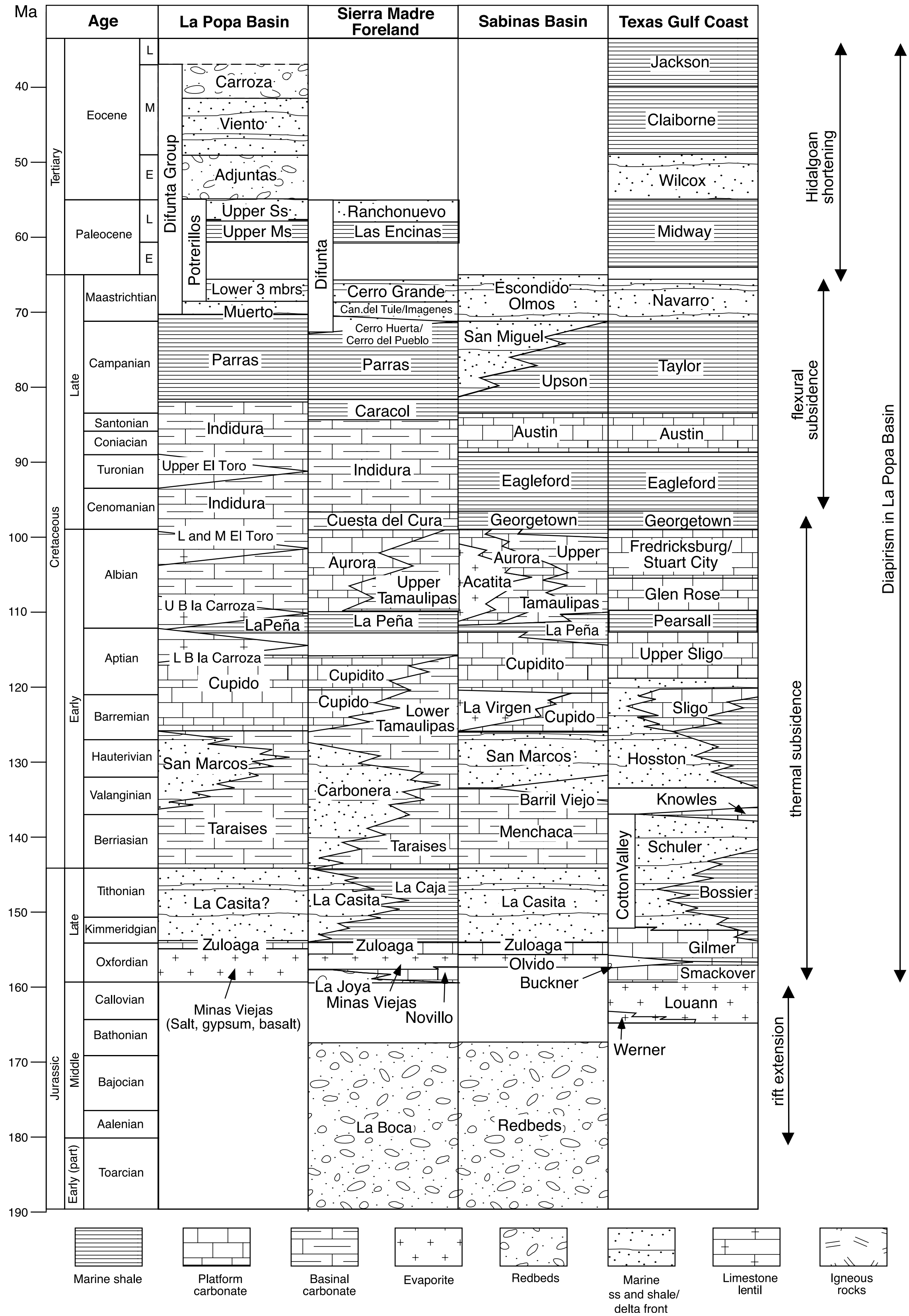

Figure 3. Generalized chronostratigraphic column for the La Popa Basin (left column) showing correlations to other basins in northeastern Mexico and the Gulf Coast. The tectonic history of the La Popa Basin is shown on the right, as well as the estimated timing of diapiric salt rise (modified from Lawton et al., 2001).

pathways by which migrated hydrocarbons, if present, came to be located along the weld.

By characterizing the system using the approach described above, a better understanding of salt weld-hydrocarbon interaction is available to apply in similar salt-related systems that lack subaerial exposure, such as those found in the subsurface of the nearby Gulf of Mexico. Salt structures are prevalent in much of the Gulf of Mexico shelf and slope environments and strongly influence the hydrocarbon systems of many fields that are in differing stages of production and exploration (Weimer et al., 1998). Globally, many other petroliferous basins are affected by salt tectonics; therefore, a better understanding of the weld in the La Popa Basin and its associated hydrocarbons should aid in predicting migration along salt welds in other basins impacted by salt tectonics.

BACKGROUND

Regionally extensive evaporites of the Minas Viejas Formation were deposited during the Late Jurassic when the La Popa Basin was initially developing as a rift, or pull-apart, basin (Giles and Lawton, 1999). Once the Minas Viejas Formation was deposited and subsequently buried by younger sediments, salt diapirism initiated within the basin (Lawton and Giles, 1997). Later in the basin's history, the latest Cretaceous to Eocene Hidalgoan orogeny caused significant crustal shortening resulting in large folds within a foreland basin setting (Guzman and de Cserna, 1963; Gray et al., 2001; Lawton et al., 2001). This orogeny was mostly responsible for the modern structure of the basin, producing anticlines and deforming strata in salt-withdrawal basins (Wolleben, 1977; Lawton and Giles, 1997).

The strata contained within the basin are primarily marine and are dominated by basinal and shallow-marine, tidal, and deltaic deposits, which show an overall progradation throughout the basin's history (Lawton et al., 2001; Murillo-Muneton and Dorobek, 2003) (Figure 3). Carbonate lithologies dominate the Late Jurassic to early Late Cretaceous parts of the section, whereas the latest Cretaceous through Eocene strata are dominantly composed of clastic lithologies. The shift from a carbonate depositional system to a clastic depositional system in the Late Cretaceous was the result of uplift to the west, which created a source for the clastic sediments that were deposited in the La Popa Basin (Cantu-Chapa, 2001; Dickinson and Lawton, 2001; Lawton et al., 2001). The only nonmarine strata present in the basin are redbeds of the Eocene Carroza Formation, which consist of sandstone, mudstone, and paleosols (Lawton et al., 2001; Buck et al., 2003). The Carroza is interpreted to contain fluvial channel and associated overbank sediments deposited in a salt-withdrawal basin (Lawton et al., 2001). The current sedimentary fill of the La Popa Basin has a thickness of 5–7 km (3.1–4.3 mi), and an estimated 5–7 km (3.1–4.3 mi) of sediment has been removed by erosion based on fission track, fluid inclusion, and vitrinite reflectance (R_o) analyses (Gray et al., 2001).

The basin history has been divided into four major tectonic stages: rifting, thermal subsidence, flexural subsidence, and Hidalgoan shortening (Lawton et al., 2001) (Figure 3). Following Hidalgoan shortening, a period of nondeposition and erosion persisted within the basin, and the only preserved strata younger than the Eocene Carroza Formation are Quaternary deposits.

METHODOLOGY

Field Work: Sample Collection

Samples were collected in and around the La Popa Basin for different reasons: to determine the presence or absence of hydrocarbons along the weld, to identify effective source rocks within the basin, and to construct a thermal history of the basin using R_o data. Observations were made along much of the length of the weld in an effort to locate areas of potential hydrocarbon migration. Samples were collected in areas that showed signs of possible hydrocarbon alteration, such as the presence of sulfur in association with gypsum, yellow-brown waxy-appearing soil, and discoloration or remineralization at the surface (Schumacher, 1996). Possible evidence of migrated hydrocarbons was observed within the remnant gypsum salt, along the interface

Table 1. Geochemical Results from Background Samples, Potential Migrated Hydrocarbon Samples, and Effective Source Rock Samples*

Sample location	Sample Id.	TOC	S1	S2	S3	T_{max} (°C)	HI	OI	S1/TOC	PI
Background Carroza Samples										
Carroza	01MO04	0.22	0.01	0.02	0.11		9	50	5	0.33
Carroza	05LP6	0.19	0.00	0.00	0.05		0	26	0	
Potential Migrated Samples										
Weld	01MO05	1.06	0.27	0.21	0.50	514	20	47	25	0.56
Weld	02LP01	0.59	0.34	0.06	0.00	395	10	0	58	0.85
Weld	02LP03	0.10	0.02	0.00	0.46	m	0	460	20	1.00
Weld	02LP04	0.09	0.02	0.01	0.45	m	11	479	21	0.67
Weld	02LP09	0.17	0.01	0.03	0.12	423	18	71	6	0.25
Weld	03LP13	0.08	0.02	0.01	0.06	335	12	73	24	0.67
Weld	03LP14	0.06	0.01	0.01	0.06	410	17	105	17	0.50
Weld	03LP16	0.18	0.07	0.05	0.36	340	28	200	39	0.58
Weld	03LP22	0.02	0.01	0.01	0.02	466	50	100	50	0.50
Weld	03LP32	0.18	0.03	0.05	0.10	399	28	56	17	0.37
Weld	03LP35	0.09	0.00	0.00	0.38	m	0	422	0	
Weld	05LP3	0.88	0.17	0.05	0.24	357	6	27	19	0.77
Weld	05LP5	0.76	0.06	0.05	0.57	355	7	75	8	0.55
Boca la Carroza	01MO08	0.12	0.01	0.01	0.72	m	8	600	8	0.50
Portrerillos	03LP15	0.08	0.02	0.02	0.06	421	26	78	26	0.50
Carroza	03LP23	0.12	0.04	0.06	0.12	434	50	100	33	0.40
Carroza	03LP24	0.41	0.15	0.02	0.10	298	5	24	36	0.88
Carroza	03LP31	0.16	0.02	0.06	0.16	456	37	99	12	0.25
Carroza	02LP02	0.24	0.01	0.00	0.12	m	0	49	4	1.00
Carroza	03LP12	0.08	0.03	0.06	0.25	362	72	301	36	0.33
Effective Source Rock Samples										
Upper Potrerillos	02LP06	0.51	0.03	0.01	0.00	333	2	0	6	0.75
Upper Potrerillos	02LP05	0.47	0.02	0.00	0.26	m	0	55	4	1.00
Upper Potrerillos	01MO06	0.66	0.03	0.03	0.16	399	5	24	5	0.50
Upper Potrerillos	01MO07	0.47	0.01	0.02	0.09	386	4	19	2	0.33
Parras	01MO11	0.14	0.02	0.02	0.10	335	14	71	14	0.50
Parras	03LP33	0.24	0.02	0.02	0.13	335	8	55	8	0.50
Parras	03LP34	0.20	0.03	0.02	0.04	362	10	20	15	0.60
Parras	01MO11	0.14	0.02	0.02	0.10	335	14	71	14	0.50
Aurora	01MO10	0.13	0.00	0.01	0.09	m	8	69	0	0.00
Indidura	03LP30	0.07	0.01	0.02	0.19	298	27	255	13	0.33
Taraises	03LP28	0.01	0.00	0.00	0.00	m	0	0	0	
Taraises	01MO01	0.15	0.02	0.02	0.16	452	13	107	13	0.50
La Casita	03LP27	0.33	0.17	0.02	0.12	m	6	36	51	0.89
La Casita	03LP26	0.30	0.10	0.04	0.14	338	13	47	33	0.71
La Casita	01MO03	0.18	0.03	0.02	0.02	m	11	11	17	0.60
Zuloaga	01MO02	0.13	0.01	0.03	0.00	m	23	0	8	0.25

*Total organic carbon (TOC) reported as weight percent (wt.%); S1, S2, and S3 refer to the sequential peaks released during Rock-Eval analysis; S1 and S2 = mg HC/g; S3 = mg CO_2/g; a calculated T_{max} value of m indicates a meaningless ratio; hydrogen index (HI) = (mg HC/g C org); oxygen index (OI) = (mg CO2/g C org); production index (PI) = S1/(S1 + S2).

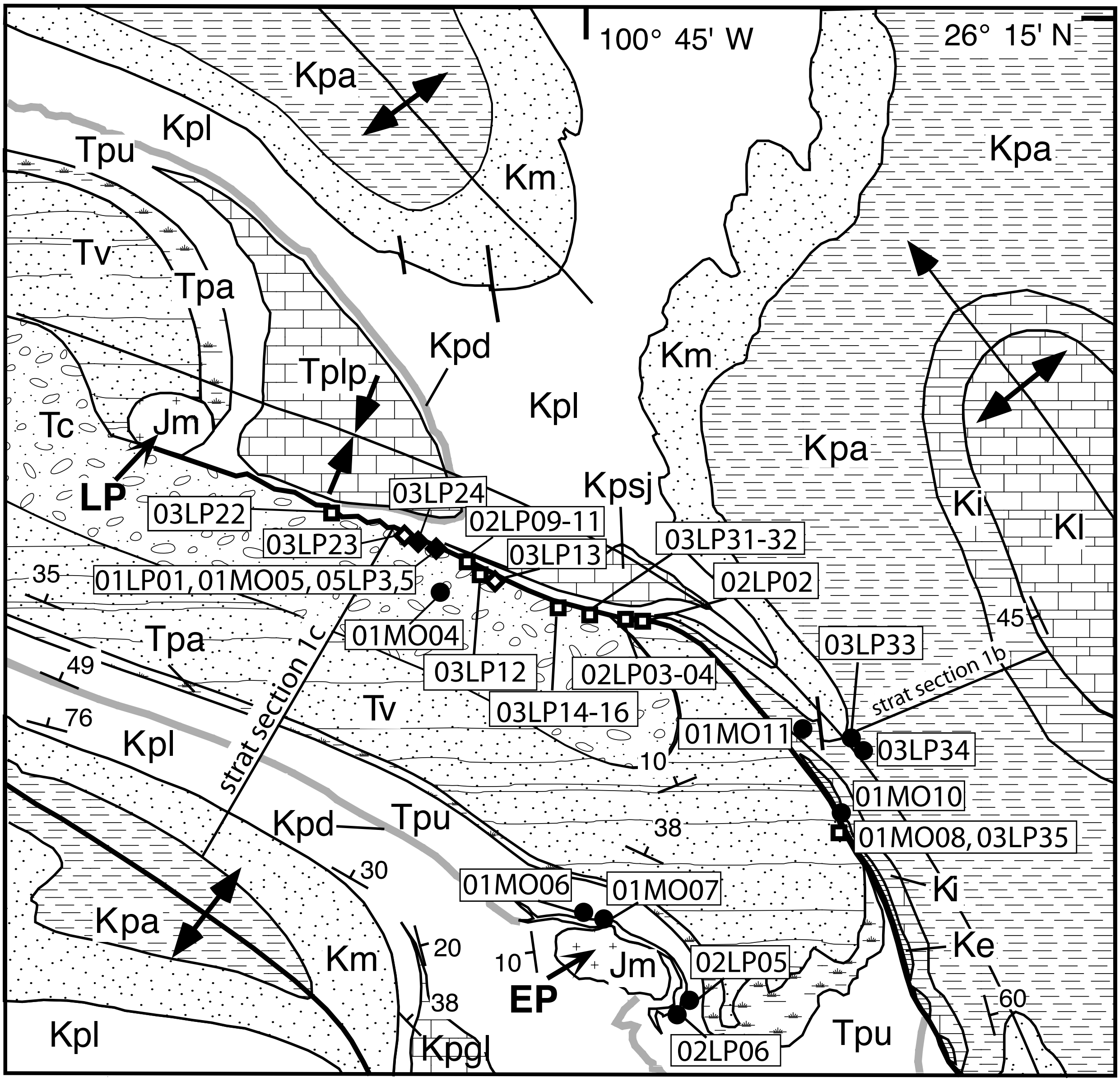

Figure 4. Map of the weld in the La Popa Basin showing where samples were collected and where stratigraphic sections were measured. Black-filled circles mark effective source rock sample sites; source rock samples not shown on the map were collected from older stratigraphy that does not crop out in the La Popa Basin. Localities with filled diamonds have geochemical indications of hydrocarbons; locations with open diamonds smelled like crude oil in the field but have low geochemical values; and locations with open squares indicate sites that are altered but have neither a hydrocarbon odor nor elevated geochemical levels. The upper two (of three) stratigraphic section locations are shown; the basal stratigraphic section measured older Cretaceous limestones exposed slightly off of the map farther to the southeast within the core of the Minas Viejas anticline. Symbols and unit designations are the same as those in Figure 2 (modified from Lawton et al., 2001). Measured stratigraphic sections 1b and 1c are discussed in the text.

between the salt and adjacent lithologies southwest of the weld, and within lithologies just southwest of the weld. Twenty samples (Table 1, second group) that showed suggestions of hydrocarbon migration were collected along the weld (Figure 4).

To search for effective source rocks within the La Popa Basin, stratigraphic units between the Jurassic Minas Viejas Formation and the Eocene Carroza Formation were examined in an attempt to locate organic-rich lithologies. Black shales and carbonates that visually appeared to be organic rich were collected for screening as effective source rock candidates (Figure 4). Some samples are from the Minas Viejas anticline, which lies to the east of

Table 2. Measured Vitrinite Reflectance Values for Samples Collected in and around the La Popa Basin*

Vitrinite Reflectance Results			
Sample No.	Formation	Measured R_o	Description
Upper Section, in Carroza Mini-basin			
03LP40	Carroza	0.93	Mudstone, top of Carroza
01MO04	Carroza	0.92	Mudstone, mid. Carroza
03LP41	Carroza	0.91	Mudstone, basal Carroza
03LP21	Adjuntas	1.01	Mudstone, top of Adjuntas
03LP20	Adjuntas	Barren	Mudstone, basal Adjuntas
01MO06	Upper Potrerillos	1.09	Mudstone, base upper Potrerillos
03LP19	Upper Potrerillos	1.13	Mudstone, base upper Potrerillos
03LP18	Lower Potrerillos	1.35	Mudstone, top lower Potrerillos
03LP17	Lower Potrerillos	1.47	Mudstone, middle lower Potrerillos
03LP38	Lower Potrerillos	0.76	Mudstone, base lower Potrerillos
Middle Section, Northeast of the Weld			
03LP39	Muerto	0.95	Mudstone, near the top of the Muerto
01MO11	Parras	0.93	Mudstone, upper Parras
03LP33	Parras	1.47	Mudstone, upper Parras
Lower Section, from Minas Viejas Section			
03LP29	Indidura	Barren	Mudstone, near top of Indidura
03LP30	Indidura	Barren	Marly mudstone, lower Indidura
03LP26	La Casita	Barren	Limestone, lower La Casita

*All samples are listed in stratigraphic order (youngest to oldest from the top of the table to the bottom).

the La Popa Basin and contains older parts of the stratigraphic section that are not exposed at the surface in the La Popa Basin. Sixteen potential effective source rocks were collected for subsequent analysis (Table 1, third group).

Finally, 16 samples for R_o analysis were collected while measuring stratigraphic sections to determine the current maturity of basin strata (Table 2). Most of the samples were collected from fine-grained clastic lithologies ($n = 13$), but an additional set of three carbonate samples were collected in the hope that they might contain sufficient vitrinite material for analysis. The carbonate samples were taken from the lower part of the section, which lacks significant clastic sediments. Samples were collected from strata ranging in age from Jurassic to Eocene in an effort to construct a fairly comprehensive thermal history profile for the basin. The complete vitrinite data set is contained in Hudson (2004).

A complete stratigraphic section was measured (above salt) for the La Popa Basin. This was done in a series of three sections: one within the Carroza minibasin southwest of the weld (1c on Figure 4), one immediately east of the basin (northeast of the weld) (1b on Figure 4), and a third section (1a, not shown on Figure 4) within the Minas Viejas anticline southeast of the basin. As the section was measured, gross lithologic characteristics were recorded to construct the stratigraphic column. The gross lithology, thickness of units, and existing age control were used to create a geohistory diagram for the La Popa Basin, and R_o data were added to model the subsidence and thermal history using BasinMod 1-D.

Total Organic Carbon and Rock-Eval

Total organic carbon (TOC) analyses employing the pyrolysis plus combustion products method (Peters and Cassa, 1994) were performed on selected samples. The results are reported as weight percentages and document the relative organic richness of samples

(Peters, 1986). Rock-Eval analyses were also performed on samples to determine whether the organic material was in situ or whether it migrated into the sample (Peters, 1986).

To screen samples we suspected of having migrated hydrocarbons, we applied the following criteria. First, they had to have higher TOC values than background samples as revealed by their TOC content. Concentrations did not have to be large but had to be enriched in organic content in comparison to surrounding lithologies. Second, samples that had elevated amounts of organic carbon had to have a Rock-Eval S1 peak greater than the corresponding S2 peak. This is commonly an indication that more organic carbon is present within the pore space of the sample than could have been generated in situ, thus indicating that at least some organic material migrated into the rock from an exterior source (Peters, 1986). Samples that satisfied these criteria were considered candidates for containing migrated hydrocarbons and were further tested using molecular organic geochemistry.

Effective source rock samples were also analyzed using TOC and Rock-Eval analytical techniques as previously outlined. When attempting to identify effective source rocks, an S2 peak larger than the associated S1 value is generally indicative of in-situ organic material (Peters, 1986) although degraded bitumens and tars can appear as S2 hydrocarbons. Also, the quality of organic material within the various effective source rocks was determined using Rock-Eval analysis. Production index (PI), hydrogen index (HI), and oxygen index (OI) were used to estimate the generation of hydrocarbons from effective source rocks and to assess the quality of organic material (HI versus OI) within the various samples (Espitalié et al., 1977).

Molecular Organic Geochemistry

Based on preliminary geochemical results, samples containing elevated TOC and encouraging Rock-Eval results were further analyzed using molecular organic geochemistry. Samples were crushed using a clean mortar and pestle into particles with a diameter less than approximately 3 mm (0.11 in.) then divided into two groups: samples thought to contain migrated hydrocarbons, and possible source rock samples. For the potential migrated hydrocarbon samples, a soft extraction was done to promote dissolution of organic material from the pore spaces of the sample. For the effective source rock samples, a more standard extraction was performed (Peters et al., 2005a). Samples were analyzed on an HP gas chromatography (GC) using a standard program. For samples that showed n-alkanes on the GC traces, the saturate fractions were run on an HP GC-mass selective detector (MSD) operated in single-ion monitoring mode, scanning for the following mass-to-charge ratios: *m/z* 177, 191, 217, 218, 231, and 259. Full details of the methodology and program parameters can be found in Hudson (2004).

DATA AND DISCUSSION

Evidence of Migrated Hydrocarbons

Data and Discussion

The TOC percentages of the samples collected along the weld range from 0.06 to 1.06 (Table 1). Measured Rock-Eval parameters are also shown in Table 1. Several of the samples show an S1 value greater than the corresponding S2 value.

Based on the TOC and Rock-Eval results, six samples from along the weld (02LP01, 02LP02, 03LP16, 03LP24, 03LP31, and 03LP32) were chosen for further analysis at Stanford's molecular organic geochemistry laboratory. These samples generally had elevated TOC values and S1 values higher than the S2 values. All six samples were analyzed using GC and mass spectroscopy. Figure 5 shows two of the six gas chromatograms for these samples, with several of the major n-alkane peaks labeled. The two samples shown in Figure 5, 03LP31 and 03LP32, show peaks indicative of normal alkanes, plus pristane (Pr) and phytane (Ph). The chromatograms for these samples show compounds ranging from n-C_{14} to n-C_{36}, with peaks maximizing between n-C_{16} and n-C_{20}. The Pr/Ph ratios of 1.6 and 2.0, respectively, were calculated for samples 03LP31 and 03LP32. The full suite of n-alkanes in these samples indicates that they are not biodegraded. Because these are surface samples, they

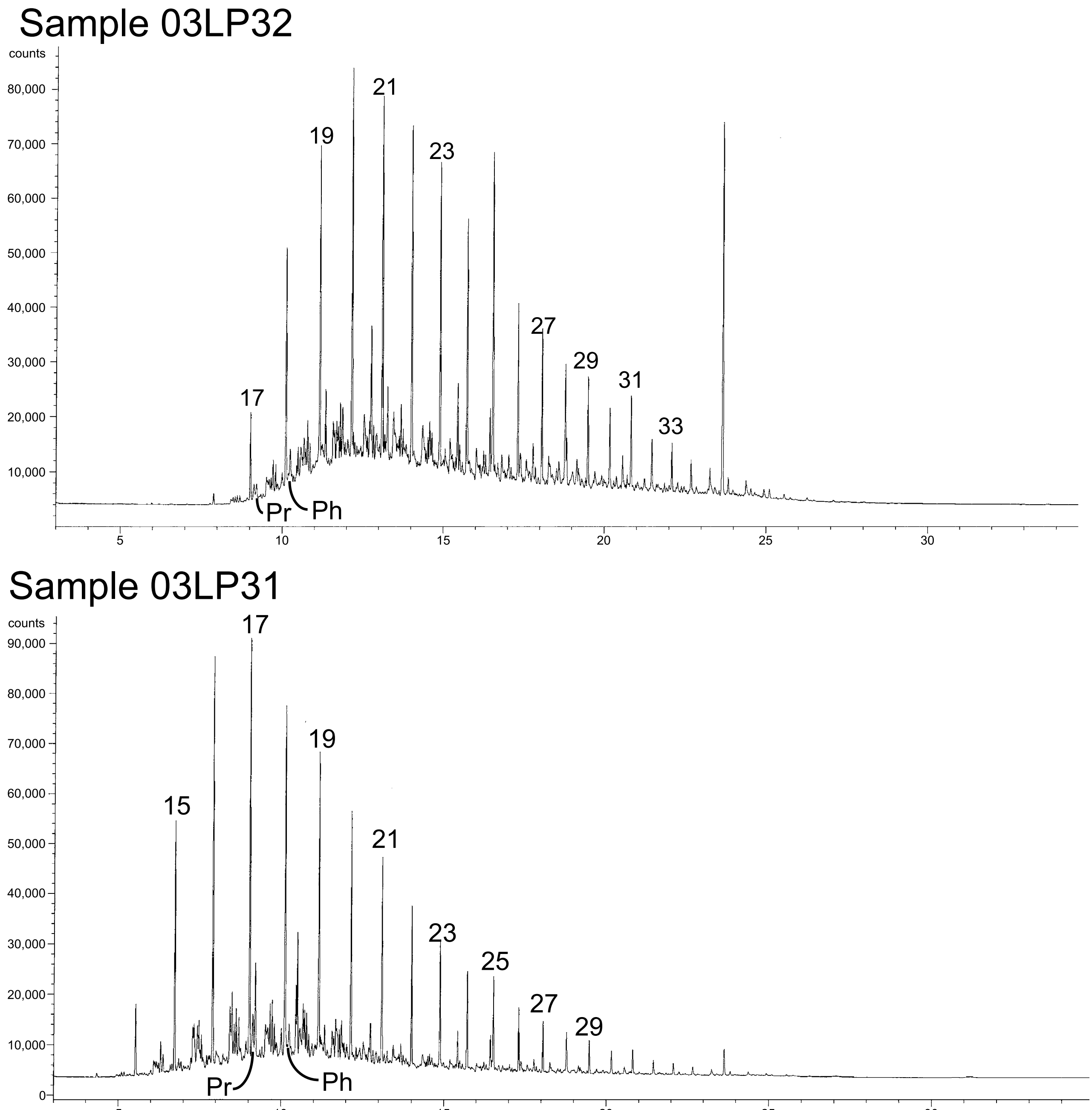

Figure 5. Gas chromatograms for samples 03LP31 and 03LP32, which were collected from along the weld, indicating the presence of migrated hydrocarbons. Several n-paraffins as well as pristane and phytane are labeled. Pr = pristane; Ph = phytane.

must be the result of an active migration that is ongoing today. The n-alkanes are absent in the other four samples, and peaks such as Pr/Ph are difficult to resolve. The elevated baseline and low signal-to-noise ratios of these samples suggest that they have undergone biodegradation at or near the surface (Palmer, 1993). Samples 03LP16 and 03LP24 produced GC traces with very low signal-to-noise ratios, and biomarker peaks are not resolvable. For this reason, interpretations were not attempted using these samples.

The same six samples were also analyzed using a GC-MSD, and several of the resulting chromatograms are shown in Figure 6. Although all samples yielded a low signal-to-noise ratio, many biomarkers can be identified. The diasterane/sterane and

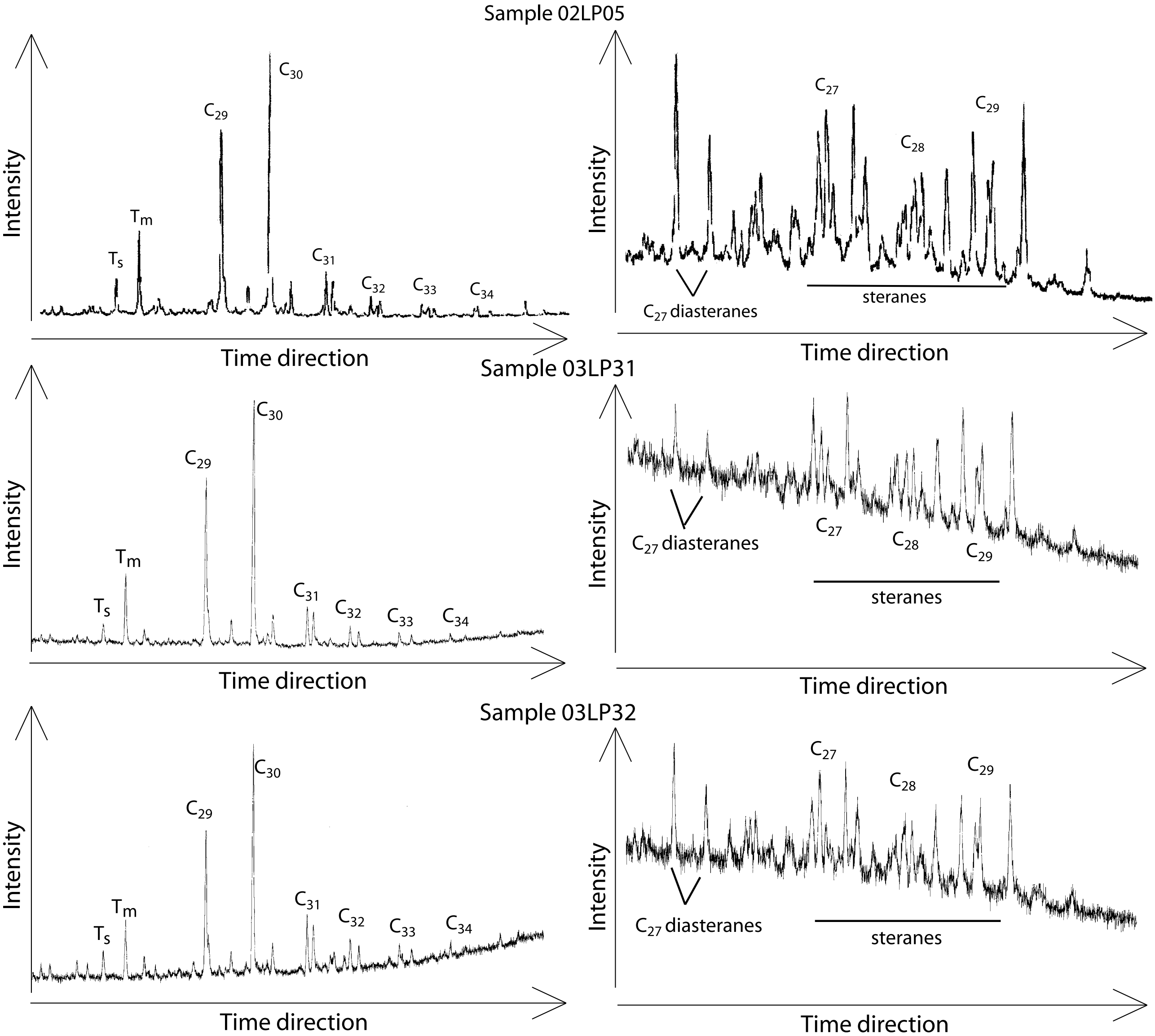

Figure 6. The *m*/*z* 191 and 217 traces from the upper Portrerillos mudstone source rock (upper traces) and two migrated samples collected along the weld, showing similar biomarkers. T_s = 18a(H)-22, 29, 30 trisnonneohopane; T_m = 17a(H)-22, 29, 30 trisnorhopane.

diahopane/hopane ratios are elevated suggesting a clay-rich source rock (Rubenstein et al., 1975; Sieskind et al., 1979), and the homohopanes decrease from C_{31} to C_{35} (C_{33} to C_{35} are not resolvable in most samples), suggesting a source rock deposited in suboxic conditions (Ten Haven et al., 1988). In all samples, the T_s/T_m (18a (H)-22, 29, 30-trisnonneohopane/ 17a(H)-22, 29, 30-trisnorhopane) ratios, tricyclic/ 17α-hopane ratios, and n-alkane envelope style are indicative of mature oils, although some variability from sample to sample exists (samples 02LP01 and 03LP32 seem to be less mature than the other samples based on higher pentacyclic/tricyclic ratios) (Seifert and Moldowan, 1978; Peters et al., 2005b).

Various ratios were calculated to compare the samples taken along the weld in the La Popa Basin to one another, such as the relative abundance of the C_{27}, C_{28}, and C_{29} steranes. This ratio is frequently used for correlation of hydrocarbon samples because these biomarkers are commonly well preserved through the processes of hydrocarbon generation and migration and are determined by characteristics of the original organic material (Peters et al., 2005b). All samples are very similar, with average values of

36% C_{27}, 26% C_{28}, and 38% C_{29} and standard deviations of 3%, 1%, and 3%, respectively, suggesting that these samples could be genetically related.

Sixteen effective source rock samples were analyzed using TOC and Rock-Eval, and the results of these analyses are shown in Table 1. The TOC values range from 0.01 to 0.66 wt.%, with an average value of 0.26 wt.%. Four of the five highest values are from the upper mudstone member of the Potrerillos Formation with TOC values that range from 0.47 to 0.66 wt.%. Measured Rock-Eval values for 17 of the samples are low and not indicative of good source rock quality (Table 1), and many samples do not show a convincing S2 > S1 relationship (Peters and Cassa, 1994).

Four of the 18 effective source rock samples were selected, based on TOC and Rock-Eval results, for further study using molecular organic geochemistry. Samples 02LP05, 02LP06, 03LP30, and 03LP33 were analyzed using GC and mass spectrometry. These samples are all organic lean, and GC analyses showed that none of the samples yielded a regular n-paraffin envelope. However, GC-MSD analysis showed that diasterane/sterane and diahopane/hopane ratios were elevated, and relative homohopane abundances decreased from C_{31} to C_{35}, similar to what was seen in the migrated samples as mentioned above. The tricyclic/pentacyclic ratio differed from sample to sample, with sample 03LP33 appearing dissimilar to the other samples. This parameter is mainly used as an indicator of maturity but can be used in source rock–migrated material correlation as well. The relative abundance of the C_{27}, C_{28}, and C_{29} steranes was also determined for use in oil-source rock correlation. The samples show a range of values, with an average of 40% C_{27}, 26% C_{28}, and 35% C_{29}, with standard deviations of 2, 6, and 2%, respectively. These ratios and others were used to attempt an oil-source rock correlation for the La Popa Basin.

Most of the alteration we observed was in close association with the Carroza Formation. We measured TOC values for typical, unaltered Carroza mudstones to assess their background level of organic carbon to compare them with altered samples. Two Carroza samples were analyzed for this purpose and had TOC values of 0.19 and 0.22 wt.%. Two other samples from within the Carroza Formation (samples 03LP12 and 03LP23) showed evidence of remineralization and/or discoloration but yielded TOC values of 0.08–0.12 wt.% (Table 1). We therefore assume that the average TOC value for unaltered strata of the Carroza Formation is generally about 0.20 wt.% or less. Consequently, samples with TOC values lower than 0.20 wt.% were not considered to contain migrated hydrocarbons.

The geochemical data indicate the occurrence of migrated hydrocarbons along the weld. Samples with (1) TOC values above 0.2 wt.%, (2) S1 peaks greater than the corresponding S2 peaks, and (3) recognizable hydrocarbon biomarkers are considered to contain migrated hydrocarbons. This includes samples 01MO05, 02LP01, 03LP24, 05LP3, and 05LP5; see Figure 4 for the sample locations.

Generally speaking, the values for S1 and S2 peaks are low. However, several samples suspected of containing migrated material do have S1 peaks greater than their S2 peaks as expected. However, other samples show an S2 > S1 relationship, which does not directly support the idea that they contain migrated hydrocarbons. Samples 02LP01, 03LP24, 01MO05, and 05LP3 show S1 values significantly higher than the corresponding S2 values, which supports the idea that at least some of the organic material within these samples migrated from an external source (Peters and Cassa, 1994).

Distinctive biomarkers were found in most of the selected samples using molecular organic geochemistry. These include n-alkanes, steranes, and terpanes (e.g., Figures 5, 6). One sample (03LP16) lacked convincing biomarkers. If this sample ever contained migrated hydrocarbons, they have been altered to the point that biomarker analysis yielded no meaningful results. Such alteration would likely be the result of biodegradation, which frequently occurs at or near the surface and is characterized by the removal of n-alkanes and a large naphthene envelope in the gas chromatograph (Peters et al., 2005a). A second possibility is that the sample never contained migrated hydrocarbons. Although apparent biodegradation is most evident in sample 03LP16, samples 02LP01, 02LP02, and 03LP24 also show signs of biodegradation (low yield of n-alkanes, characteristic baseline pattern). Despite apparent biodegradation, however, these three samples yielded recognizable sterane and terpane biomarkers.

Based on the results of biomarker analysis, the migrated hydrocarbons found along the weld in the La Popa Basin appear to have a common origin. Comparison of the chromatograms suggests this in a qualitative way, as shown by the similarity of the results in Figures 5 and 6. Comparison of the five migrated samples, based on the relative percentages of C_{27}, C_{28}, and C_{29} steranes, shows this in a more quantitative way, with the relative abundances of the steranes in the five samples being very similar. Additional biomarker ratios that match well in all samples are the C_{35} hopane/C_{31}–C_{35} homohopane ratio and several of the diasterane/sterane ratios. Based on the similar biomarker content, it seems that they are likely from a single source and constitute one oil family. The biomarker distributions are consistent with a mature oil.

The presence of migrated hydrocarbons along the weld in the La Popa Basin demands that an effective source rock, which had been or is still generating in the La Popa Basin, is present. Our TOC and Rock-Eval analyses show that most samples collected are currently of poor source potential. Although these samples are organically lean, they may have been an effective source rock for the basin in the past, and their present-day low amounts of organic material are the result of advanced thermal maturity. Samples from the upper mudstone member of the Potrerillos Formation have biomarkers that are very similar to the migrated material along the weld, and we propose that the upper mudstone member of the Potrerillos Formation is a potential source rock for the migrated hydrocarbons. Although the migrated samples have a range of maturity (samples 02LP01 and 03LP32 seem to be less mature than the other samples), all of the samples have biomarker ratios consistent with mature oil. This interpretation is based on several calculated biomarker ratios such as C_{32} 22S/(C_{32} 22S + 22R) hopanes (Ensminger et al., 1977) and $T_s/(T_s + T_m)$ ratios. Poor preservation of C_{34} and C_{35} hopanes within the samples suggests that the source rock was suboxic; these biomarkers are related to bacterial activity in the depositional environment (Peters et al., 2005b). A very slight suggestion of carbonate input is observed, shown by the relative height of C_{24} tetracyclic terpanes (Connan et al., 1986), but other biomarker ratios (e.g., diasterane/sterane, Pr/Ph, C_{35} homohopane) are consistent with derivation from a shale source rock. The Pr/Ph ratios are between 1 and 3, suggesting that the source rock was likely deposited in a suboxic setting. The large relative amount of C_{29} steranes compared to C_{27} and C_{28} steranes suggests terrestrial organic input (Talukdar et al., 1986). Based on these observations, it appears that a suboxic, mature marine shale was likely the source rock that generated the hydrocarbons found along the weld. Thus, the biomarker evidence eliminates most of the lower part of the stratigraphic section in the basin because it is dominated by carbonates. Possibly, marine shales of limited aerial extent exist in the source kitchen within the lower part of the stratigraphy and served as source rocks for the migrated hydrocarbons, but their presence is purely speculative. None of the sequence stratigraphy studies conducted in the basin suggest such shales, but because the subsurface is undocumented, we cannot rule out the possibility of their existence.

Our evidence suggests that vertical hydrocarbon migration was enhanced by diapirism along the La Popa salt weld. Hydrocarbon alteration was commonly found 0–3 m (0–10 ft) from the weld in sandy carrier beds, which were vertically oriented because of halokenetic processes, i.e., within A-type halokinetic sequences (Giles and Lawton, 2002). In addition, alteration was found along the weld in localities of complete salt removal and along the salt-sediment contact in areas with remnant salt, suggesting that the weld itself acted as a conduit to vertical fluid flow.

The presence of abundant alteration along the weld combined with obvious biomarkers in only a few altered samples can be interpreted in different ways. It may suggest that a nonbiomarker containing alteration was produced by nonhydrocarbon bearing fluids, e.g., basinal brines. Alternatively, hydrocarbons may have been present during the alteration event but have subsequently been completely removed by degradation. If some or all of the nonbiomarker-bearing alterations seen in the field were produced by migrating hydrocarbons, which have subsequently been degraded, it implies that

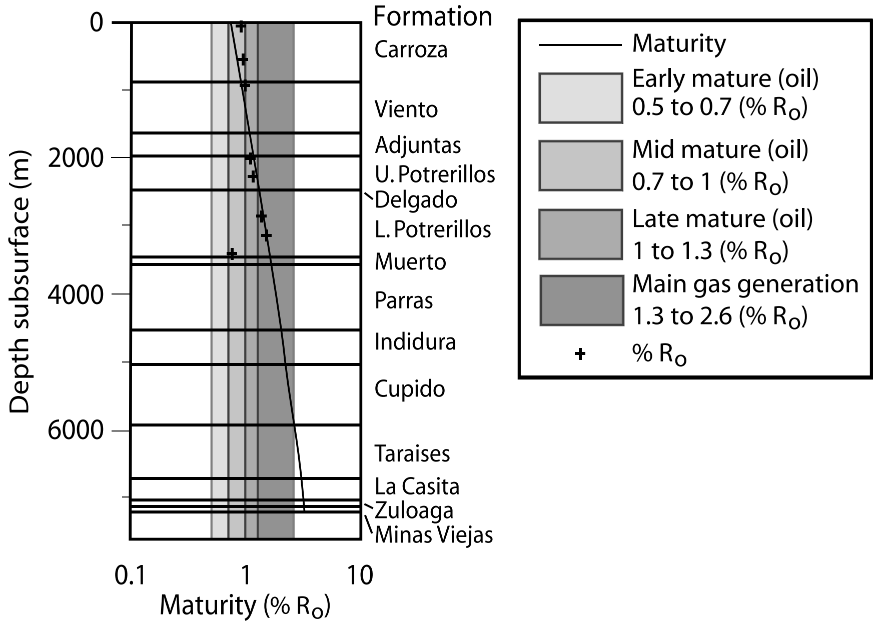

Figure 7. BasinMod 1-D plot showing measured vitrinite reflectance (R_o) (crosses) versus calculated R_o (solid line). The calculated R_o was modeled using lithology and unit thickness data determined from our measured sections. The model assumes a removed overburden of 7 km (4.3 mi) and a geothermal gradient of 15°C/km.

active hydrocarbon migration turned on and off along different parts of the weld at different times. This interpretation implies that migration along welds is complicated and difficult to constrain.

Thermal History of the La Popa Basin

Data and Discussion

The timing of hydrocarbon generation and migration within the La Popa Basin required the determination of the thermal history of the basin. Vitrinite samples keyed into the stratigraphy were collected while measuring the three stratigraphic sections (Figure 7). Results of the analyses were used to constrain the thermal history of the La Popa Basin and calibrate a basin model. The model also considers the apatite-fission track analysis (AFTA) and fluid inclusion data of Gray et al. (2001) and a new sensitive high-resolution ion microprobe (SHRIMP) age for the Carroza of 55 Ma ± 1 (T. Lawton, 2008, personal communication). Of the 17 samples collected for vitrinite analysis, 13 of them yielded sufficient quantities of material (Table 2). Overall, the samples show a decrease in R_o from the base of the section up to the Carroza Formation. However, some samples do not follow this trend. This is likely because of the complex structure of the region; lateral variations in burial are likely because of Hidalgoan shortening (Gray et al., 2001).

The vitrinite samples were collected in two groups: a group from north of the weld, which covers the lower part of the stratigraphic section (La Casita-Muerto formations), and a group from the salt-withdrawal mini-basin south of the weld covering the Potrerillos-Carroza formations (Table 2). Several samples collected north of the weld are from the several samples are from the Indidura and La Casita formations, but these samples are from carbonate-dominated strata and did not yield vitrinite material. Two samples were collected from the Parras Shale, and these samples yielded R_o values of 1.47 and 0.93%. Although these values are based on greater than 15 measurements each, a large difference is observed between the R_o values yielded for the two samples. This disparity is not easily explained because the two samples were collected from the same area and is problematic for basin modeling. The final sample collected north of the weld is from the Muerto Formation, and this sample yielded an R_o value of 0.95%. This is a higher value than the 0.93% reported for the Parras Shale sample, which is stratigraphically below the Muerto Formation. Based on the disparity between R_o values for the Parras Shale, the small number of samples that yielded R_o data, and the lack of a predictable trend of decreasing values moving up through the stratigraphy, the data set from the north of the weld was not used for basin modeling.

Higher in the stratigraphy, most of the samples collected south of the weld are from along one continuous stratigraphic section (Figure 4). The first sample is from the basal lower mudstone member of the Potrerillos Formation, and it yielded an R_o value of 0.76%. This value is not in good agreement with the reported values for samples stratigraphically above it. The rest of the samples from the lower mudstone member of the Potrerillos Formation up through the Carroza Formation show a steady decrease from higher values (1.47% for the lower mudstone member of the Potrerillos Formation) to lower values up through the section, with a minimum R_o value of 0.91% within the Carroza Formation. With the exception of the sample collected from the basal Potrerillos Formation, the samples from this group show a consistent pattern of decreasing R_o values upsection. Also, this data set is much more complete than the one from samples collected north of the weld. For this reason, the vitrinite data from this sample group were used for basin modeling.

Variable overburdens and heat-flow values were tested until a good match between modeled and measured R_o values was found (Figure 7). In general, the model matches measured reflectance values best when using an overburden of 7 km (4.3 mi) and a geothermal gradient of 15°C/km (higher heat-flow values made the slope of the line in Figure 7 much too flat). Based on the measured R_o values and basin modeling results, eight of the samples reached the peak oil generation stage. Two samples reached the late oil generation stage, and the remaining two reached the main gas generation stage, with a maximum reflectance value of 1.47%. According to the basin model, the oldest strata of the Jurassic Zuloaga Formation entered the oil window about 100 Ma, and the Eocene Carroza Formation entered the oil window about 45 Ma (Figure 8), just prior to uplift. The basin underwent variable subsidence from the Jurassic through the Eocene, and a period of rapid subsidence in the Paleogene immediately preceded a period of uplift that began about 40 Ma (Figure 8). Generation is presumed to have terminated soon after uplift initiated (Katz et al., 1988). The subsidence curve produced through basin modeling is steep shortly after basin initiation in the Jurassic, shows a concave-up shape through the early Late Cretaceous, a concave-down shape for the remainder of the Cretaceous, and a separate concave-down segment into the Paleogene (Figure 8).

Because lithologies younger than the Eocene Carroza Formation are not preserved within the basin, we relied on the results of Gray et al. (2001) to constrain the timing of deposition and subsequent removal of materials that previously were deposited upon the Carroza Formation. In a regional study of Mexico with a limited number of samples from the La Popa Basin, Gray et al. (2001) estimated that 5–7 km (3.1–4.3 mi) of overburden once existed above the Carroza Formation, with major uplift and erosion starting about 36 Ma and reaching peak rates in the Oligocene and early Miocene.

To get our model to match our vitrinite data, we used a geothermal gradient of 15°C/km and an eroded overburden of 7 km (4.3 mi). Our modeled heat flows are much lower than the 30°C/km estimated by Gray et al. (2001) but are required to match our vitrinite data. The data set used for this study is more extensive than previous studies and shows agreement with the more regional study conducted by Gray et al. (2001) in that both models predict approximately 7 km (4.3 mi) of overburden, which has since been removed. An important inference we draw from the different calculated geothermal gradients is that the low geothermal gradient we employed may be specific to the salt-withdrawal basin in La Popa where the high thermal conductivity of the salt may have kept sediments within the salt-withdrawal minibasin at anomalously low temperatures caused by wicking effects. Additionally, high sedimentation rates would have suppressed the geothermal gradient within the minibasin, and then maximum maturity levels would have been locked in once the basin began to invert and never had a chance to equilibrate to the regional geothermal gradient.

The basin subsidence curve shown on Figure 8 can be used to interpret the cause of subsidence during different times within the La Popa Basin. When observing this curve, a concave-up curve indicates a gradual decline in the rate of subsidence thought to represent thermal subsidence, whereas

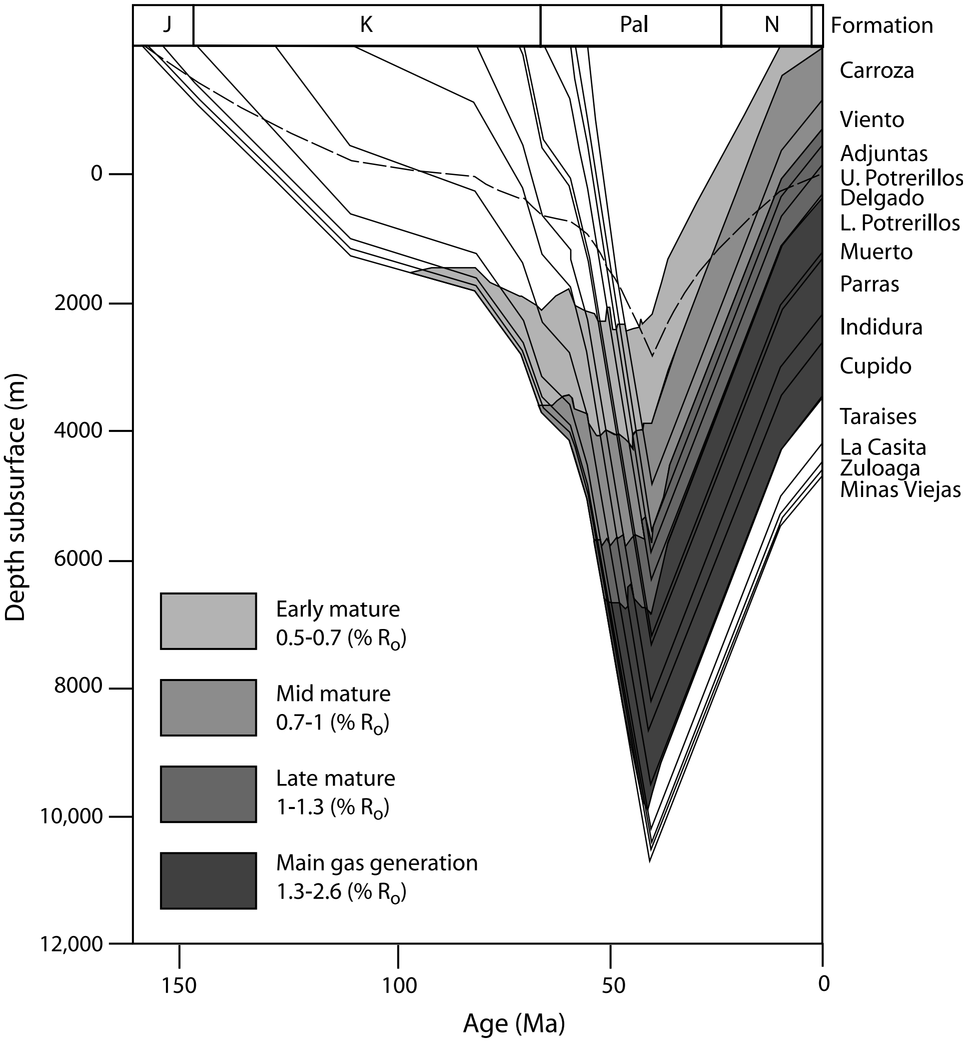

Figure 8. BasinMod 1-D geohistory diagram, showing the subsidence and uplift of the basin through time. Also shown are the various stages of maturation, allowing the prediction of onset of hydrocarbon generation for various effective source rocks within the basin. The tectonic subsidence curve is also shown. R_o = vitrinite reflectance.

a concave-down curve represents an increase in subsidence thought to represent the tectonic subsidence of the basin (Dickinson, 1976). Using these guidelines, our model can be compared to the tectonic history of the basin as outlined by Dickinson and Lawton (2001) and Lawton et al. (2001). As shown in Figure 3, the basin is thought to have undergone rifting during deposition of the Minas Viejas and Zuloaga formations (Lawton et al., 2001). Within the basin model (Figure 8), this is represented by the initial steep angle of the subsidence curve during the Late Jurassic. Following rifting in the basin came a period of thermal subsidence (Figure 3), which persisted from the Late Jurassic into the early Late Cretaceous (Lawton et al., 2001). This is also shown in the basin model (Figure 8) by the concave-up shape of the subsidence curve during this time. According to Lawton et al. (2001), the remainder of the Late Cretaceous was characterized by flexural subsidence of the basin (Figure 3), and the concave-down shape of the subsidence curve represents the tectonically driven subsidence during this time (Figure 8). Starting in the early Tertiary, Hidalgoan shortening affected the area (Dickinson and Lawton, 2001; Lawton et al., 2001), again causing tectonically driven basin subsidence, and this can be seen by the convex-down shape of the subsidence curve during the first half of the Paleogene (Figure 8). Finally, the geohistory diagram shows the uplift and removal of 7 km (4.3 mi) of Eocene and younger strata between approximately 36 Ma and the present (Figure 8), which was established through a series of sensitivity analyses compared to the R_o data from this study and thermal history studies previously performed in the La Popa Basin (Gray et al., 2001).

The agreement between Figure 8 and the tectonic history outlined by Dickinson and Lawton (2001), Gray et al. (2001), and Lawton et al. (2001) further validates this model of the La Popa Basin.

CONCLUSIONS

Hydrocarbon migration has occurred along the weld in the La Popa Basin, as revealed by geochemical analysis of samples from along much of its length. Eighteen samples were collected, mostly from the western half of the weld, and 10 show evidence of enrichment in organic carbon content based on TOC analysis. Rock-Eval analysis confirms that at least some of this material has migrated from an external source, and molecular organic geochemistry has shown the presence of distinct biomarkers. The presence of these materials requires a source rock within or proximal to the basin. The upper mudstone member of the Potrerillos Formation has many geochemical properties that are similar to the migrated hydrocarbons along the weld but currently lacks organic carbon of sufficient quality to account for the migrated material along the weld. However, the lack of organic richness may be because of its thermal maturity ($R_o = 1.13$). Biomarkers found in the migrated material along the weld indicate that the source rock that generated the hydrocarbons was deposited in a suboxic, clay-rich, marine environment; a finding in agreement with our supposition that the upper mudstone member of the Potrerillos Formation is a likely source rock that generated the oil.

Basin modeling provides insight into the thermal and subsidence histories of the basin. Burial was rapid at first and continued without major interruptions until about 40 Ma (Lawton et al., 2001). Many of the basin lithologies reached thermal conditions sufficient for hydrocarbon generation fairly early in the basin's history at a time when more salt was likely present along the weld in the La Popa Basin. Basin modeling also indicates that significant erosion (about 7 km [4.3 mi] worth of sediment) has occurred post-Eocene. An apparently anomalously low geothermal gradient for the La Popa Basin compared to regional geothermal gradients is assumed to be the result of the high thermal conductivities of the salt in the basin and high sedimentation rates during the foreland basin development stage of basin evolution.

All samples that contained migrated hydrocarbons from along the weld were located along the southern side of the weld, presumably sourced from down-dropped, more deeply buried strata south of the weld. Given that the presumed source rock, the upper mudstone member of the Potrerillos Formation, does not exist to the north of the weld, the discovery of migrated hydrocarbons only on the south side of the weld may reflect more on the distribution of the source rock than it does upon any impact the weld may have had on migration. Despite that limitation of our results, migrated hydrocarbons appear to be restricted to localities that have type-A halokinetic sequences as defined by Giles and Lawton (2002). This association has important implications for hydrocarbon exploration near salt structures.

REFERENCES CITED

Buck, B. J., T. F. Lawton, D. Merkler, R. A. Howley, S. Khtesat, Z. Rawajfih, B. Waidmann, and A. Hanson, 2003, Snowballs in the Devil's Anus and other adventures in the world of pedogenic sulfates: Geological Society of America Abstracts with Programs, v. 35, p. 257.

Cantu-Chapa, A., 2001, The Taraises Formation (Berriasian–Valanginian) in northeastern Mexico: Subsurface and outcrop studies, *in* C. Bartolini, R. T. Buffler, and A. Cantu-Chapa, eds., The western Gulf of Mexico Basin: Tectonics, sedimentary basins, and petroleum systems: AAPG Memoir 75, p. 219–240.

Connan, J., J. Bouroullec, D. Dessort, and P. Albrecht, 1986, The microbial input in carbonate-anhydrite facies of a sabkha paleoenvironment from Guatemala: A molecular approach: Organic Geochemistry, v. 10, p. 29–50, doi:10.1016/0146-6380(86)90007-0.

Dickinson, W. R., 1976, Plate tectonic evolution of sedimentary basins: AAPG Continuing Education Course Note Series 1, 62 p.

Dickinson, W. R., and T. F. Lawton, 2001, Carboniferous to Cretaceous assembly and fragmentation of Mexico: Geological Society of America Bulletin, v. 113, p. 1142–1160, doi:10.1130/0016-7606(2001)113<1142:CTCAAF>2.0.CO;2.

Ensminger, A., P. Albrecht, G. Ourisson, and B. Tissot, 1977, Evolution of polycyclic alkanes under the effect of burial (early Toarcian shales, Paris Basin), *in* R. Campos and J. Goni, eds., Advances in organic geochemistry: Madrid, Enadimsa, p. 45–52.

Espitalié, J. M., M. Madec, B. Tissot, J. J. Mennig, and P. Leplat, 1977, Source rock characterization method for petroleum exploration: Proceedings of the 9th Annual Offshore Technology Conference, p. 439–448.

Giles, K. A., and T. F. Lawton, 1999, Attributes and evolution of an exhumed salt weld, La Popa Basin, northeastern Mexico: Geology, v. 27, p. 323–326, doi:10.1130/0091-7613(1999)027<0323:AAEOAE>2.3.CO;2.

Giles, K. A., and F. F. Lawton, 2002, Halokinetic sequence stratigraphy adjacent to the El Papalote diaper, northeastern Mexico: AAPG Bulletin, v. 86, p. 823–840.

Gray, G. G., R. J. Pottorf, D. A. Yurewicz, K. I. Mahon, D. R. Pevear, and R. J. Chuchla, 2001, Thermal and chronological record of syn- and post-Laramide burial and exhumation, Sierra Madre Oriental, Mexico, *in* C. Bartolini, R. T. Buffler, and A. Cantu-Chapa, eds., The western Gulf of Mexico Basin: Tectonics, sedimentary basins, and petroleum systems: AAPG Memoir 75, p. 159–181.

Guzman, E. J., and Z. de Cserna, 1963, Tectonic history of Mexico, *in* O. E. Childs and B. W. Beebe, eds., Backbone of the Americas—Tectonic history from pole to pole: AAPG Memoir 2, p. 113–129.

Hudson, S. M., 2004, Hydrocarbon occurrences within the La Popa Basin: Potential source rocks, thermal maturation, and hydrocarbon migration along the La Popa salt weld, La Popa Basin, NE Mexico: Master's thesis, University of Nevada Las Vegas, Las Vegas, Nevada, 142 p.

Katz, B. J., R. N. Pheifer, and D. J. Schunk, 1988, Interpretation of discontinuous vitrinite reflectance profiles: AAPG Bulletin, v. 72, p. 926–931.

Lawton, T. F., and K. A. Giles, 1997, El Papalote diapir, La Popa Basin, *in* K. Soegaard, F. Vegas, and T. Lawton, eds., Structure, stratigraphy and paleontology of Late Cretaceous–early Tertiary Parras-La Popa foreland basin near Monterrey, northeast Mexico: AAPG Field Trip Guidebook 10, p. 55–74.

Lawton, T. F., K. A. Giles, F. J. Vega, and C. Rosales-Dominguez, 2001, Stratigraphy and origin of the La Popa Basin, Nuevo Leon and Coahuila, Mexico, *in* C. Bartolini, R. T. Buffler, and A. Cantu-Chapa, eds., The western Gulf of Mexico Basin: Tectonics, sedimentary basins, and petroleum systems: AAPG Memoir 75, p. 219–240.

McBride, B. C., P. Weimer, and M. G. Rowan, 1998, The effect of allochthonous salt on the petroleum systems of northern Green Canyon and Ewing bank (offshore Louisiana), northern Gulf of Mexico: AAPG Bulletin, v. 82, p. 1083–1112.

Murillo-Muneton, G., and S. L. Dorobek, 2003, Controls on the evolution of carbonate mud mounds in the Lower Cretaceous Cupido Formation, northeastern Mexico: Journal of Sedimentary Research, v. 73, p. 869–886, doi:10.1306/043003730869.

Palmer, S. E., 1993, Effect of biodegradation and water washing on crude oil composition, *in* M. H. Engel and S. A. Macko, eds., Organic geochemistry: New York, Plenum Press, p. 511–533.

Peters, K. E., 1986, Guidelines for evaluating petroleum source rock using programmed pyrolysis: AAPG Bulletin, v. 70, p. 318–329.

Peters, K. E., and M. R. Cassa, 1994, Applied source rock geochemistry *in* L. B. Magoon and W. G. Dow, eds., The petroleum system—From source to trap: AAPG Memoir 60, p. 93–120.

Peters, K. E., C. C. Walters, and J. M. Moldowan, 2005a, The biomarker guide: Biomarkers and isotopes in the environment and human history: Cambridge, Cambridge University Press, v. 1, 471 p.

Peters, K. E., C. C. Walters, and J. M. Moldowan, 2005b, The biomarker guide: Biomarkers and isotopes in petroleum exploration and earth history: Cambridge, Cambridge University Press, v. 2, 1155 p.

Pritchett, J. A., and W. M. House, 1998, Analysis of allochthonous salt and salt welds in the northern Gulf of Mexico utilizing 3D seismic data: AAPG Bulletin, v. 82, p. 1954.

Rowan, M. G., 2004, Do salt welds seal?: 24th Annual Gulf Coast Section SEPM Foundation Bob F. Perkins Research Conference, Program and Abstracts, p. 18.

Rubenstein, I., O. Siesking, and P. Albrecht, 1975, Rearranged steranes in a shale: Occurrence and simulated formation: Journal of the Chemical Society, Perkin Transaction 1, p. 1833–1836.

Schumacher, D., 1996, Hydrocarbon-induced alteration of soils and sediments *in* D. Schumacher and M. A. Abrams, eds., Hydrocarbon migration and its near-surface expression: AAPG Memoir 66, p. 71–89.

Seifert, W. K., and J. M. Moldowan, 1978, Applications of steranes, terpanes, and monoaromatics to the maturation, migration, and source of crude oils: Geochimica et Cosmochimica Acta, v. 42, p. 77–95, doi:10.1016/0016-7037(78)90219-3.

Sieskind, O., G. Joly, and P. Albrecht, 1979, Simulation of the geochemical transformation of sterols: Superacid effects of clay minerals: Geochimica et Cosmochimica Acta, v. 43, p. 1675–1679, doi:10.1016/0016-7037(79)90186-8.

Snyder, F. C., and J. A. Nugent, 1996, Teak; a complex subsalt trap geometry, south Timbalier Block 260, northern Gulf of Mexico (abs.): AAPG Annual Convention Official Program, v. 5, p. A132.

Talukdar, S., O. Gallango, and M. Chin-A-Lien, 1986, Generation and migration of hydrocarbons in the Maracaibo Basin, Venezuela: An integrated basin study: Organic Geochemistry, v. 10, p. 261–279, doi:10.1016/0146-6380(86)90028-8.

Ten Haven. H. L., J. W. de Leeuw, J. S. Sinninghe Damsté, and P. A. Schenck, 1988, Application of biological markers in the recognition of paleohypersaline environments, *in* A. J. Fleet, K. Kelts, and M. R. Talbot, eds., Lacustrine petroleum source rocks: London, Blackwell, p. 123–130.

Weimer, P., J. R. Crews, R. S. Crow, and P. Varnai, 1998, Atlas of petroleum fields and discoveries, northern Green Canyon, Ewing bank, and southern Ship shoal and south Timbalier areas (offshore Louisiana), northern Gulf of Mexico: AAPG Bulletin, v. 82, p. 878–917.

Wolleben, J. A., 1977, Paleontology of the Difunta Group (Upper Cretaceous–Tertiary) in northern Mexico: Journal of Paleontology, v. 51, p. 373–398.